Possible Uses of Rapid Switching Devices and Induction RF for an LHC Upgrade

F. Zimmermann, CERN, Geneva, Switzerland

Abstract

The European Accelerator Network on High Energy High Intensity Hadron Beams (CARE HHH) is studying scenarios for LHC Luminosity and enegry upgrades. The upgrade options considered foresee either the compensation of long-range beam-beam collisions by pulsed electromagnetic wires, which may be realized via fast switches, or the use of crab cavities. Both the wire pulser and the crab rf system could benefit from the technological advances of induction rf devices. In addition, the generation of superbunches represents a possible use of induction rf for an LHC upgrade, promising high luminosity at moderate total beam current. While the present LHC detectors cannot handle the event pile up implied by this type of beam, superbunches remain an attractive solution for a proposed linac-ring electron-proton collider based on LHC and CLIC, the so-called QCD Explorer.

INTRODUCTION

The Large Hadron Collider (LHC) now under construction at CERN is the world's next energy-frontier machine. It will collide two proton beams with a centre-of-mass energy of 14 TeV (7 times the energy of the Tevatron's proton-antiproton collisions) at design and ultimate luminosities of 10^{34} cm^{-2}s^{-1} and 2.3×10^{34} cm^{-2}s^{-1} (about 100 times that of the Tevatron). The start of the LHC ring commissioning is scheduled for the fall of 2007, and the first physics run expected in spring 2008. Figure 1 shows the overall layout of the LHC, with two proton beams circulating in separate pipes and crossing each other at the four detectors of the two high-luminosity experiments ATLAS and CMS, the B physics experiment LHC-B, and the ion-collision experiment ALICE, respectively.

Since several years, we are already considering possible upgrade paths for this unique facility; see, e.g., Ref. [2]. More recently, the LHC luminosity upgrade has become the primary focus of the CARE ("Coordinated Accelerator Research in Europe") [3] HHH network [4], which is supported within the 6th Framework Programme of the European Union. The parallel development of higher field magnets (for an eventual LHC energy upgrade) is the objective of a separate European Joint Research Activity, called NED ("Next European Dipole") [5].

This report is organized as follows. We first describe the general framework and strategy of the LHC upgrade. Then we look at new higher-energy injectors. Stronger dipole magnets and various interaction-region choices are addressed in the following two sections. Proceeding, we discuss long-range beam-beam compensation using wires and, next, crab cavities. Lastly, the merits and drawbacks of superbunches and their possible use at a QCD Explorer are examined. The reports concludes with a summary and outlook.

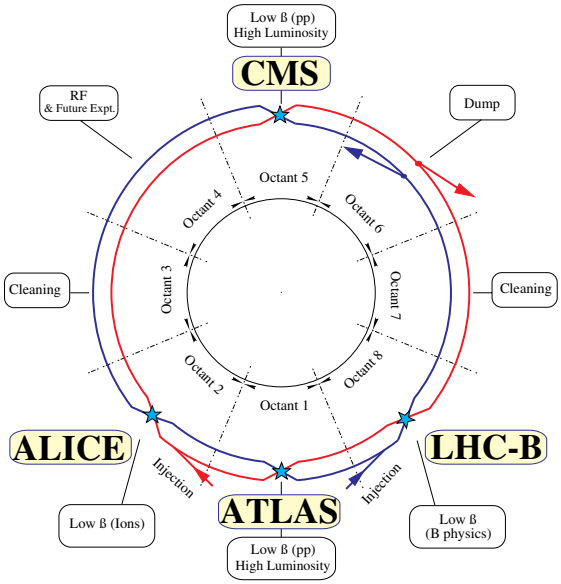

Figure 1: Layout of the LHC with its four interaction points [1].

Many of the developments discussed, e.g., the higher-energy injectors, long-range beam-beam compensation using a pulsed electromagnetic wire, rf crab cavities, superbunches or the QCD Explorer, may profit from recent progress in induction-rf technologies, which has been the focus of the RPIA (Recent Progress in Induction Acceleration) 2006 workshop.

LHC UPGRADE

HHH

The European Accelerator Network on **H**igh Energy **H**igh Intensity **H**adron Beams (HHH) [4] was launched in 2004. The goals of this network are (1) to develop a road map for the upgrade of the European accelerator infrastructure (LHC & GSI complexes), (2) to prepare the technical realization and scientific exploitation of the upgraded facilities, and (3) to guide pertinent accelerator R&D and ex-

perimental studies. The HHH work package most closely linked to the RPIA2006 workshop is the one on Accelerator Physics and synchrotron Design (APD).

In November 2004m the first CARE-HHH-APD Workshop (HHH-2004) on 'Beam Dynamics in Future Hadron Colliders and Rapidly Cycling Synchrotrons' was held [6]. This was followed, in September 2005, by the second APD workshop (LHC-LUMI-05) on 'Scenarios for the LHC Luminosity Upgrade' [7].

Stages

A staged upgrade of the LHC is envisioned [2]. In the first stage, the LHC performance is pushed without new hardware, which should achieve the ultimate luminosity of 2.3×10^{34} cm^{-2}s^{-1} with collisions at two interaction points. After about 7 years the low-β quadrupoles need to be replaced for two reasons [8, 9]: first, it is expected that by then the first generation quadrupoles will be destroyed due to radiation damage from the collision debris, and, second, the effective further reduction of statistical errors will require higher luminosity. By means of a two times lower β^*, using the new improved quadrupoles, the luminosity is doubled to 4.6×10^{34} cm^{-2}s^{-1}. The next phase is the upgrade of the LHC injectors, which will allow, e.g., increasing the number of bunches, also by a factor of two. The luminosity is again doubled, and it may now exceed 9.2×10^{34} cm^{-2}s^{-1}. In a final step, the energy of the LHC will be increased by a factor 2–3, by installing stronger dipole magnets with a field of 15–24 T, depending on the technological progress.

Upgrade Paths and Limitations

Figure 2, from Francesco Ruggiero, illustrates the various upgrade paths in a two-dimensional space spanned by the bunch population and the number of bunches. The hyperbolae correspond to curves of constant total current. The ultimate beam-beam limit is reached for a certain bunch population, at the nominal bunch length and crossing angle. The standard upgrade simply increases the number of bunches at the beam-beam limit. This may imply a higher-harmonic rf to shorten the bunches, as the crossing angle will need to be increased in order to limit the effect of long-range collisions and to maintain a constant value for the product of crossing angle and bunch length, $(\theta_c \sigma_z)$. Two alternative upgrade scenarios, raising the luminosity at the beam-beam limit, are either to increase the bunch length and possibly reduce the number of bunches, or to increase the crossing angle [10].

The following considerations will guide the design choice. The peak luminosity at the beam-beam limit scales inversely proportional with the interaction-point (IP) beta function. The total beam intensity is likely to be limited by electron cloud, collimation, machine protection, and injectors. The minimum crossing angle depends on the beam intensity, and, at large values, it is limited by the triplet aperture. Longer bunches allow a higher value for the ratio

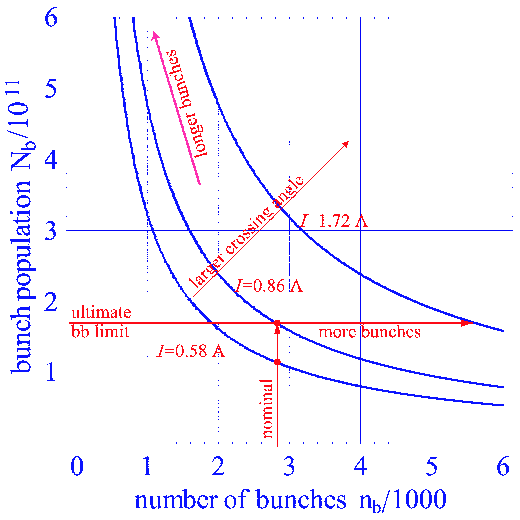

Figure 2: Schematic of LHC upgrade paths and limitations in the two-dimensional space spanned by the bunch population and the number of bunches (Courtesy F. Ruggiero).

$N_b/(\gamma\epsilon)$ if the latter is not limited by the injectors. Also, electron cloud and impedance heating will be more benign for longer bunches. If the bunches can be made flat instead of Gaussian a further $\sqrt{2}$ gain in luminosity is possible for bunches longer than β^* [10, 11]. The event pile up in the physics detectors increases with the square of the bunch population. In addition, the luminosity lifetime at the beam-beam limit depends only on β^*.

Table 1 compares the parameters of the nominal and ultimate LHC with those for two different upgrade paths, in one case embracing a larger number of shorter bunches, in the other a smaller number of longer bunches. The peaks luminosity is about the same for either upgrade path. The long bunches have the advantages of avoiding electron-cloud problems and implying only a small increase in the total beam current. Their drawback is the much higher number of pile-up events in the physics detectors.

Electron Cloud

One of the important constraints likely to determine the upgrade path eventually chosen is the electron cloud.

Figure 3 shows a schematic of the electron build-up process for the nominal LHC. First, photo-electrons are created by synchrotron radiation at the beam-pipe wall. These photo-electrons are then accelerated in the electric field of the photon-emitting bunch which passes simultaneously. The electrons gain a maximum energy of 200 eV, close to the energy where the secondary emission yield is maximum, and they hit the opposite side of the vacuum chamber after about 5 ns. Upon impact on the wall, the accelerated primary electrons generate low-energy secondary electrons, which may stay inside the beam pipe until the following bunch arrives, 25 ns behind the previous one.

Table 1: Parameters for the nominal and ultimate LHC compared with those for two upgrade scenarios with (1) shorter bunches at 12.5-ns spacing [baseline], (2) longer more intense uniform bunches at 75-ns spacing [large Piwinski parameter], including heat loads per beam aperture.

parameter	symbol	nominal	ultimate	shorter bunches	longer bunches
protons/bunch	N_b [10^{11}]	1.15	1.7	1.7	6.0
no. bunches	n_b	2808	2808	5616	936
bunch spacing	$\Delta t_{\rm sep}$ [ns]	25	25	12.5	75
average current	I [A]	0.58	0.86	1.72	1.0
norm. transv. emittance	$\gamma\epsilon$ [μm]	3.75	3.75	3.75	3.75
longit. profile		Gaussian	Gaussian	Gaussian	flat
rms bunch length	σ_z [cm]	7.55	7.55	3.78	14.4
beta function at IP1&5	β^* [m]	0.55	0.5	0.25	0.25
full crossing angle	θ_c [μrad]	285	315	445	430
Piwinski parameter	$\phi \equiv \theta_c \sigma_z/(2\sigma^*)$	0.64	0.75	0.75	2.8
peak luminosity	L [10^{34} cm^{-2}s^{-1}]	1.0	2.3	9.2	8.9
events per crossing		19	44	88	510
IBS growth time	$\tau_{x,\rm IBS}$ [h]	106	72	42	75
nucl. scattering lumi lifetime	$\tau_{\rm N}/1.54$ [h]	26.5	17	8.5	5.2
lumi lifetime ($\tau_{\rm gas} = 85$ h)	τ_L [h]	15.5	11.2	6.5	4.5
effective luminosity ($T_{\rm turnaround} = 10$ h)	L [10^{34} cm^{-2}s^{-1}]	0.4	0.8	2.4	1.9
optimum run duration	$T_{\rm run,opt}$ [h]	14.6	12.3	8.9	7.0
effective luminosity ($T_{\rm turnaround} = 5$ h)	L [10^{34} cm^{-2}s^{-1}]	0.5	1.0	3.3	2.7
optimum run duration	$T_{\rm run,opt}$ [h]	10.8	9.1	6.7	5.4
average e-cloud heat load at 4.6–20 K in the arc for $R = 50\%$ and $\delta_{\rm max} = 1.4$ (in parentheses for $\delta_{\rm max} = 1.3$)	$P_{\rm e-cloud}$ [W/m]	1.07 (0.44)	1.04 (0.59)	13.34 (7.85)	0.26 (0.26)
synchrotron radiation heat load at 4.6–20 K	P_γ [W/m]	0.17	0.25	0.50	0.29
image current power at 4.6–20 K	$P_{\rm ic}$ [W/m]	0.15	0.33	1.87	0.96
beam-gas scattering heat load at 1.9 K for 100-h beam lifetime (in parentheses for 10 h lifetime); it is assumed that elastic scattering ($\approx 40\%$ of total cross section) leads to local loss	$P_{\rm gas}$ [W/m]	0.038 (0.38)	0.056 (0.56)	0.113 (1.13)	0.066 (0.66)

The secondary electrons are then accelerated by the field of this bunch, producing new secondary electrons in turn. The repetition of this process leads to an avalanche-like generation of electrons, which is also know as 'beam-induced multipacting'. The build up of electrons only saturates when the electron space-charge field prevents further secondary electrons from penetrating into the inside of the vacuum chamber.

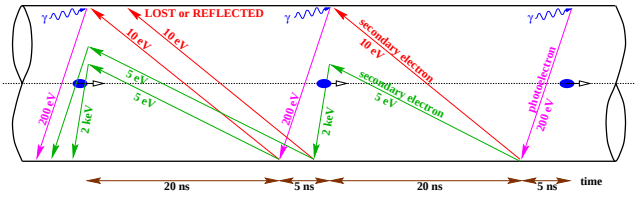

Figure 3: Schematic of electron-cloud build up in the vacuum chamber for the nominal LHC. Primary electrons are generated on the chamber wall illuminated by synchrotron radiation via photoemission. The number of electrons is then amplified exponentially by beam-induced multipacting (Courtesy F. Ruggiero).

Both simulations and numerous experiments suggest that the electron cloud build becomes worse for shorter bunch spacing. Displayed in Fig. 4 are the bunch populations for which an electron-cloud effect is observed at various accelerators, as a function of the bunch spacing [15]. Both axes are drawn in a logarithmic scale. Data for positron as well as hadron storage rings are included. For a large class of storage rings the threshold bunch population seems to scale roughly linearly with the bunch spacing:

$$N_b^{\rm thr} \propto \Delta t_{\rm sep} \ . \qquad (1)$$

At a spacing of 20–25 ns, the points for the SPS, PS, Tevatron with uncoalesced beam, and for the APS fall on top of each other. For the SPS, data of electron-cloud thresholds are available for three different spacings (5 n, 25 ns and 50 ns), and they exactly follow the empirical scaling of (1). Also RHIC data reveal a large sensivitity to the bunch spacing, but the observed thresholds are much lower than for the other machines. A tentative explanation is that the surfaces in RHIC may be less well conditioned, and, therefore, exhibit a larger secondary emission yield. The thresholds found at DAFNE and KEKB are looser than for the proton machines and the APS, possibly due to extensive surface cleaning by synchrotron radiation. Also shown are design operating points of several planned accelerators, namely, the nominal and ultimate LHC, and the damping rings for TESLA and CLIC. From here the LHC upgrade path could go in two different directions, either parallel to the SPS 'threshold line' towards larger spacing, longer bunches and higher intensity with $N_b \propto \Delta t_{\rm sep}$, staying at a constant distance from the electron-cloud threshold, or towards shorter bunch spacings $\Delta t_{\rm sep}$ at constant bunch intensity N_b, which would require an additional improvement in the surface conditions.

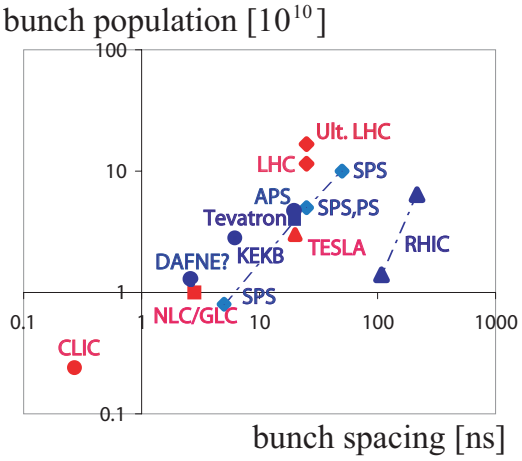

Figure 4: Electron-cloud threshold bunch intensity vs. bunch spacing observed at existing storage rings (blue) and nominal working points of several future projects (red), including the nominal and ultimate LHC [15].

For long flat bunches with large separation the electron cloud is reduced. The reason is illustrated in Fig. 5 which sketches the electron motion during the passage of a long superbunch [12, 13, 14] with nearly uniform profile. Photoelectrons generated at the head of the bunch are trapped in the increasing beam potential and released only at the end of the bunch passage. Electrons emitted at the wall during most of the bunch passage move in a quasi-static beam potential, and do not gain any net energy from the beam. They traverse the beam, being first accelerated and then decelerated, and hit the opposite side of the chamber with their original emission energy, which is too low to produce a significant amount of secondary electrons. Only electrons generated near the very tail of the bunch experience a beam potential decreasing in time and, as a result, experience a net energy gain. These electrons can therefore contribute to an amplification process, which is appropriately called 'trailing-edge multipacting' [13]. The severity of the trailing-edge multipacting depends on the detailed shape of the bunch profile. In any case, the large majority of protons in a superbunch do not participate in the multipacting process, and, therefore, the heat loads calculated for superbunches tend to be negligible, orders of magnitude below those for the nominal LHC bunched beam [14].

Upgrade Issues

The interaction regions (IRs) need to be upgraded so as to become compatible with lower β^* and higher beam current. For the new IR optics, two basic layouts can be distinguished, namely quadrupole first (as in the present LHC or Tevatron) and dipole first (as in RHIC). Heat load and damage by collision debris must be taken into account.

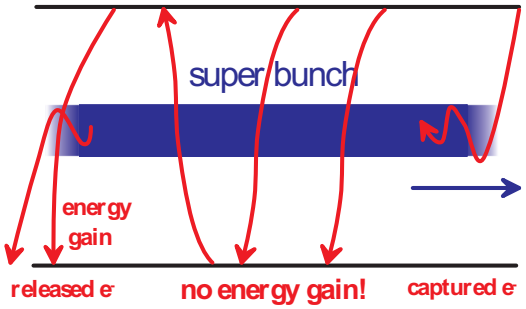

Figure 5: Schematic of reduced electron-cloud build up for a superbunch; most electrons do not gain any energy when traversing the quasi-static beam potential; and the simulated heat load is negligible (after V. Danilov [13]) [14].

Other constraints on the low-beta quadrupoles are imposed by magnet technology, required apertures, and field quality.

The crossing angle leads to a significant geometric luminosity loss, while the long-range collisions result in a reduction of dynamic aperture, which can be catastrophic if the crossing angle is chosen too small.

The electron cloud, whose build up was described in the previous subsection, can have a number of undesirable consequences, such as heat load on the inside of the superconducting magnets, vacuum-pressure rise, reduced beam lifetime or various types of beam instabilities, all of which will greatly impact operation.

There are many other considerations. The complex interdependence between the different upgrade issues is illustrated by the draft roadmap of Fig. 6.

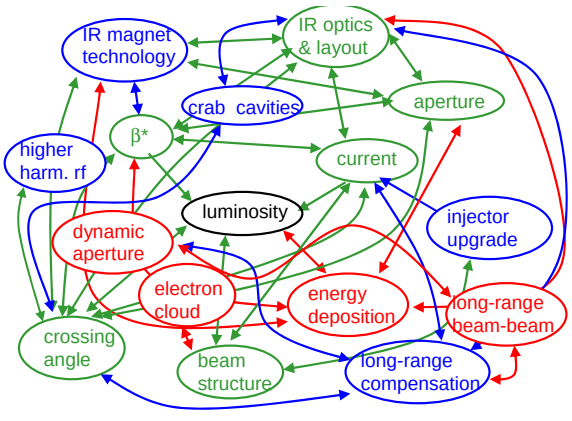

Figure 6: Upgrade roadmap for the LHC showing complex interdependence.

HIGHER-ENERGY INJECTORS

Motivations

There are several motivations for an upgrade of the LHC injectors.

First, higher-energy injectors will allow raising the LHC beam intensity (higher bunch charge, shorter bunch spacing), for limited geometric aperture. The luminosity increases in proportion to the normalized transverse emittance which can be injected into the LHC ring.

Second, dynamic changes of the magnets, like persistent currents and snapback, are reduced for higher energy. It is expected that this will improve the 'turn-around time' by a factor of 2, and the effective luminosity by about 50% (see Table 1).

A third motivation is the benefit to other CERN programmes, like neutrino physics or β beams [16].

New Injectors

The baseline injector upgrade foresees raising the SPS extraction energy from presently 450 GeV to 1 TeV in a new Super-SPS. Likewise, the top energy of the PS increases from 26 GeV to 50 GeV in a new Super PS. In parallel, the injection energy into the Super LHC goes up from 450 GeV to 1 TeV.

A Super-ISR could be an alternative to the Super PS. And a pipetron double-ring based on a superferric design [17], located in the LHC tunnel, appears to be a cost-effective alternative to the Super SPS, though a practical solution for bypassing the experimental detectors would still have to be found.

Kickers

Space constraints in the existing tunnels provide an incentive to develop more efficient kicker magnets, i.e., by improving their technology so as to reach higher deflection strength per unit. This may be an opportunity for RPIA technology. The present extraction or injection kicker parameters for PS [18], SPS [19] and LHC [20] are compiled in Table 2. A factor two increase in kicker strength would be desirable.

Table 2: Present kicker parameters [18, 19, 20].

	PS extr.	SPS extr.	LHC inj.
magnet length	0.22 m	1.674 m	2.7 m
aperture	158mm×	148(135)mm	38 mm
(diameter)	53 mm	×32(35)mm	38 mm
no. of units	4	5	4
average field	0.07 T	0.0866 T	0.111 T
flat top length	$5-12$ μs	$8-10$ μs	8 μs
flat top ripple		$<1\%$	$<0.5\%$

STRONGER DIPOLES

Motivation

Stronger dipoles are needed for increasing the beam energy. There is a good motivation of looking at higher en-

ergy. One argument is that predicting the energy for discovery is perilous. Quoting P. McIntyre [21], for a decade after the discovery of the bottom quark we knew there should be a companion top quark. Predictions of its mass over that decade grew from 20 GeV over 40 and 80 GeV to 120 GeV. Four colliders were built with top discovery as a goal and failed to produce it. Finally, the top quark was found by Fermilab at 175 GeV.

Figure 7 shows the masses of the lightest two sparticles constrained by astrophysics and cosmology, computed by Ellis et al [22]. Sparticles in the red region can only be found by the LHC energy tripler. Figure 8 displays the integrated luminosity needed for the discovery of a W-like heavy boson as a function of its energy, for two different collider energies. At masses above 3.5 TeV, doubling the beam energy is more effective than increasing the luminosity ten times.

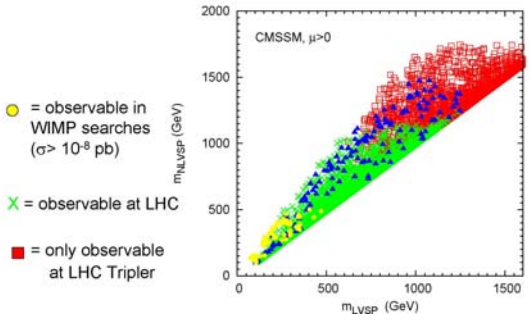

Figure 7: Mass of lightest two sparticles constrained by astrophysics and cosmology [22]. The sparticles shown in the right upper part (in red) are observable only at the LHC energy tripler [21].

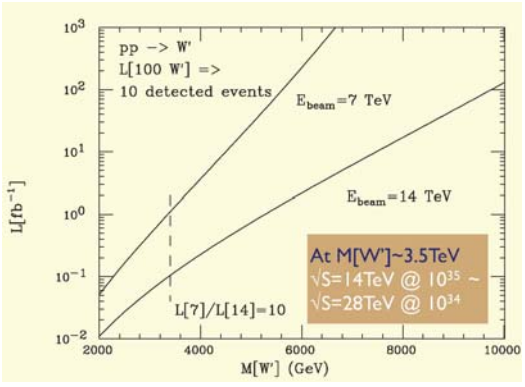

Figure 8: Production of W-like boson; at $m > 3.5$ TeV, higher energy is preferred over higher luminosity [23].

Magnet Development

The LHC beam energy is determined by the main dipole field, which nominally is 8.39 T corresponding to 7 TeV beam energy. A proof-of-principle magnet based on Nb_3Sn s.c. material at LBNL has reached 16 T a few years ago, with a 10-mm aperture [24]. The European NED activity [5] aims at developing a large-aperture (up to 88 mm), 15-T dipole-magnet model. A 24-T block-coil dipole for an LHC energy tripler is also being developed by Texas A&M University [25]. It employs high-Tc superconductor (Bi-2212) in the inner high-field windings and Ti_3Sn for the outer low-field windings. The magnet layout is illustrated in Fig. 9 and its small coil area is emphasized in Fig. 10.

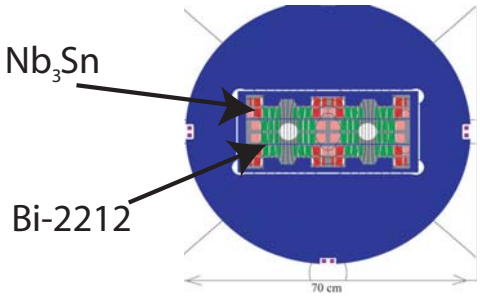

Figure 9: Schematic of a dual-pipe 24-T block dipole magnet with Bi-2122 in inner high field windings (green) and Nb_3Sn in outer low field windings (red)[21].

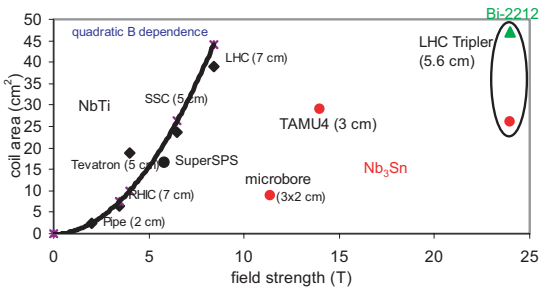

Figure 10: Magnet coil area vs. field strength for different s.c. dipoles, showing a reduced size for the proposed block-dipole magnets of the LHC energy tripler[21].

Upgraded CERN Complex

After upgrading the injectors as well as LHC itself, we arrive at the new CERN complex shown in Fig. 11, which includes Super-PS, Super-SPS, and Super-LHC. The transfer lines between Super-SPS and Super-LHC, as well as the one between Super-PS and Super-SPS, also need to be upgraded for higher field, and become 'super' transfer lines.

INTERACTION-REGION CHOICES

Candidate Solutions

During and after the LUMI-05 workshop [7], several candidate solutions for an upgraded LHC interaction-region were identified, namely

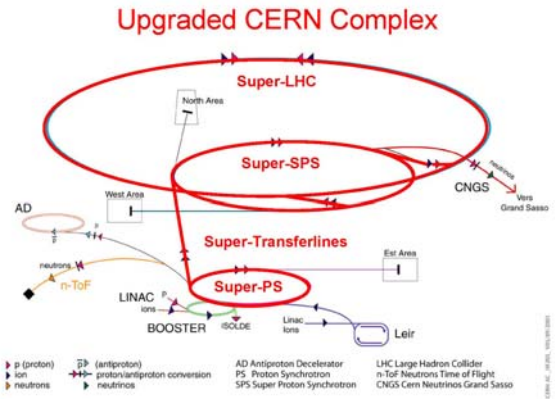

Figure 11: Schematic of upgraded CERN complex, where all rings and lines from the PS onwards are replaced by their 'super' counterparts.

- combined-function NbTi magnets with large free length from IP, l^* (O. Brüning, R. De Maria) [26];
- dipole-first options based on Nb_3Sn (R. De Maria, T. Sen, N. Mokhov) [27, 28];
- quadrupole first with Nb_3Sn (T. Sen) [28];
- quadrupole first with detector integrated dipole (J.-P. Koutchouk [29]);
- quadrupole first with flat beams (T. Sen and S. Fartoukh) [28, 30];
- quadrupole first with crab cavity (F. Zimmermann, R. Tomas) [31].

Most of these options are described and are available on newly constructed "LHC upgrade IR optics" web site [30], which will be the starting point for selecting a 'forward looking' baseline scenario. Suitable criteria for the performance rating include the (1) luminosity reach depending on energy deposition margins and shielding optimization for the IR magnets, (2) technical risks of the most critical hardware, and (3) estimated time for development, implementation and operation. Pertinent side constraints are aperture, chromatic correction, and the adapted method of long-range beam-beam compensation.

Choice of Crossing Angle

A limit on the maximum crossing angle is imposed by the luminosity reduction entailed. Figure 12 shows the geometric reduction factor

$$R_\Theta = \frac{1}{\sqrt{1+\Theta^2}}\,, \qquad (2)$$

as a function of the Piwinski angle

$$\Theta \equiv \frac{\theta_c \sigma_z}{2\sigma_x^*}\,. \qquad (3)$$

The nominal LHC parameters correspond to a Piwinski angle of $\Theta = 0.65$ and a reduction factor $R_\Theta = 0.84$. Further increases in the crossing angle result in a rapid luminosity decrease, unless the bunches can be shortened at the same time. Another limit on the maximum crossing angle arises from the aperture of the low-beta quadrupoles. The present LHC parameters are also close to this second boundary.

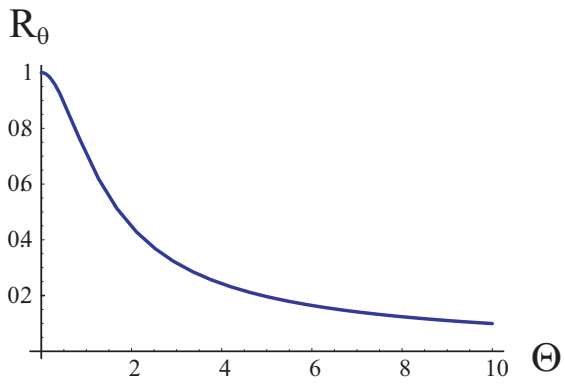

Figure 12: Geometric luminosity reduction factor R_Θ as a function of the Piwinski angle $\Theta \equiv \theta_c \sigma_z/(2\sigma_x^*)$.

On the other hand, a minimum crossing angle is required to mitigate the effect of long-range beam-beam collisions (see Fig. 13). Long-range collisions perturb the motion of protons at large betatron amplitudes, where they come close to the opposing beam. Thereby, they generate a 'diffusive' (or dynamic) aperture [32], beyond which a particle is rapidly lost. Without compensation, the minimum crossing angle imposed by the long-range beam-beam interaction is [33, 34, 35]

$$\theta_c \geq \sqrt{\frac{\epsilon}{\beta^*}}\left(\frac{d_{\rm da}}{\sigma} + 3\sqrt{\frac{k_{\rm par}}{2\times 32}\frac{N_b}{1.15\times 10^{11}}\frac{3.75\ \mu{\rm m}}{\gamma\epsilon}}\right)\,, \qquad (4)$$

where $d_{\rm da}/\sigma$ denotes the dynamic aperture in units of the rms beam size and $k_{\rm par}$ the total number of long-range collisions at the two main interaction points. Equation (4) represents a scaling law first found by Irwin [32] with numerical values inferred from the simulations of [34]. Other

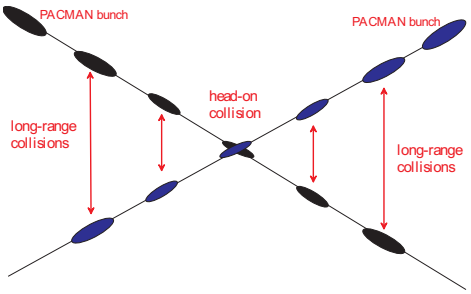

Figure 13: Schematic of long-range collisions on either side of an LHC interaction point.

simulations indicate the existence of a threshold, i.e., a few long-range encounters may have no effect on the dynamic aperture [35].

The effect of long-range collisions is a problem of increasing importance, from the SPS over the Tevatron Run-II to the LHC, *i.e.*, for operation with a larger nunber of bunches, as is illustrated by Table 3.

Table 3: Number of long-range collisions in some hadron colliders.

collider	no. of long-range encounters
SPS	9
Tevatron Run-II	70
LHC	120

Approaches for Boosting LHC Performance

Various approaches for boosting the LHC luminosity have been proposed:

- increasing the crossing angle and reducing the bunch length (higher frequency rf, e.g., 1.2 GHz, & reduced longitudinal emittance [36, 37]);
- reducing the crossing angle and applying wire compensation [38, 39, 40, 41];
- reducing the crossing angle and installing early-separation dipole 'D0' inside the detector [29];
- using crab cavities, which allow for a large crossing angle without luminosity loss [42, 43, 44, 2, 31]; the first ever demonstration of crab cavity operation in a collider is foreseen at KEKB from summer 2006;
- colliding long intense bunches with a large crossing angle [12, 10, 45].

Here RPIA technology comes into play as it could help developing solutions for a "pulsed wire compensator" [40], the crab cavities, and the super-bunches.

Baseline IR Layouts

Figure 14 displays two 'baseline' upgrade schemes. Shown on the left is an option with regular or short bunches colliding at a small crossing angle, facilitated by long-range beam-beam compensation. On the right, an alternative with crab cavities, large crossing angle and separate quadrupole channels is displayed. In this second scheme, the bunches do not need to be as short as on the left, since the crab cavities ensure de facto head-on collisions. The minimum full crossing angle required for separation into two different quadrupole channels is 2 mrad or less [46].

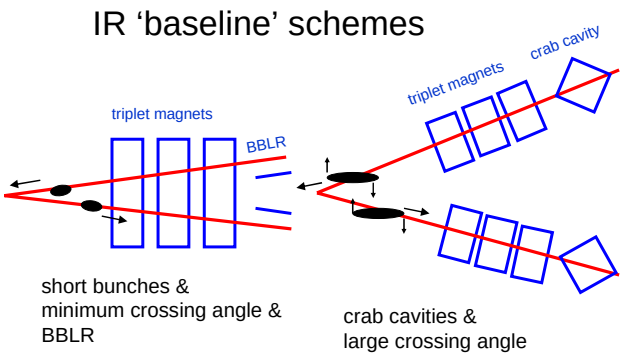

Figure 14: IR 'baseline' schemes with minimum crossing angle and possibly long-range beam-beam compensation (left) or with large crossing angle and possibly crab cavities (right); see also [9].

LONG-RANGE BEAM-BEAM COMPENSATION

Wire Compensator

The idea of compensating the effect of long-range beam-beam compensation by an electro-magnetic wire was proposed by J.-P. Koutchouk [38, 39]. The compensating wired is located roughly at the same normalized transverse distance from the closed orbit as the average distance of the counter-rotating beam at the positions of long-range encounters. Several prototype wire compensators were built at CERN and installed in the SPS, where they can be used to mimic the LHC long-range collisions and to demonstrate the compensation of each other's effect on the beam [47]. A photo of an SPS 3-wire compensator is shown in Fig. 15.

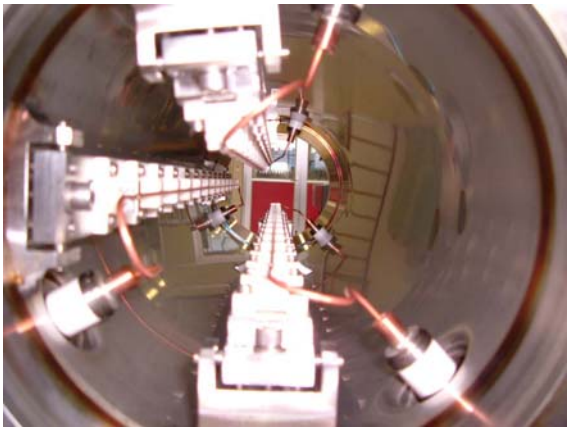

Figure 15: Photo of an SPS 3-wire compensator during assembly [47].

With only one beam in the SPS, real compensating experiments are not possible. These will be attempted at RHIC in collaboration with US-LARP [48]. The SPS and RHIC machine experiments are accompanied by extensive

long-range beam-beam simulation campaigns for the LHC, SPS, RHIC and TEVATRON, performed by various groups around the globe.

A pulsed wire would be highly attractive as it would allow effective compensation also for the bunches at the head and tail of a bunch train, so as not to degrade the lifetime of these "PACMAN" bunches. The wire pulse pattern should mimic the LHC bunch train pattern, both of which are illustrated in a compagnion paper of these proceedings. [41], where also a table with pertinent parameters can be found. The critical parameters are the high repetition rate (about 440 kHz) and the turn-by-turn amplitude and timing stability required (10^{-4} and 0.04 ns, respectively). Development of the LHC wire pulser is a topic to which RPIA technology may greatly contribute.

Merits and Plans

The following merits of wire compensation can be listed:

- long-range beam-beam compensation was demonstrated in the SPS using two wires (lifetime recovery);
- simulations predict 1–2σ gain in dynamic aperture for the nominal LHC;
- it allows keeping the same, or even smaller, crossing angle for higher beam current, thereby limiting the geometric luminosity loss to the percent level.

Further SPS experiments are planned for 2006, and, with a 3rd wire unit, in 2007. The effectiveness of compensation with real colliding beams will be tested at RHIC. We also intend to study options and feasibility of a pulsed wire by means of a laboratory test set up at CERN.

Jitter Tolerance

The turn-to-turn stability of the wire pulse is crucial. The tolerance can be estimated from theory, using a formula for the hadron-beam emittance growth due to noise excitation, including decoherence and feedback, which was derived by Alexahin [49] starting from the Vlasov equation. According to Alexahin, the relative emittance growth per turn is

$$\frac{1}{\epsilon}\frac{\Delta\epsilon}{\Delta t} \approx f_{\rm rev}\,\frac{1-s_0}{4}\,\frac{(\Delta x)^2}{\sigma_x^{*,2}}\,\frac{1}{\left(1+\frac{g}{2\pi|\xi|}\right)^2}\,, \qquad (5)$$

where g denotes a feedback gain factor (typically $g \approx 0.2$), $|\xi|$ the total beam-beam parameter (≈ 0.01), σ_x^* the horizontal IP beam size, and $s_0 \approx 0.645$ is related to the fact that only a small fraction of the energy received from a kick is imparted into the continuum eigenmode spectrum leading to an irreversible emittance growth. From formula (5), the random beam-beam offset (Δx) resulting in 1% emittance growth per hour is 1.5 nm. Without feedback ($g = 0$) the tolerance for the beam-beam random offset jitter (Δx) is 0.6 nm, for tte LHC upgrade rms IP beam size σ_x^* of 11 μm.

The beam-position jitter is related to the wire-current jitter via

$$\frac{\Delta x}{\sigma_x^{ast}} = \frac{2r_p I_w l_w}{n_{\rm IP} ecn\epsilon_N}\left(\frac{\Delta I_w}{I_w}\right)\,. \qquad (6)$$

Considering an integrated wire current strength of $I_w l_w = 120$ Am (corresponding to the compensation of 15 long-range encounters at 'ultimate' intensity), the jitter tolerance for 1% emittance growth without feedback per hour is $\Delta I_w/I_w \approx 10^{-4}$.

RF CRAB CAVITIES

History and Status

Crab cavities were first proposed for linear colliders by R. Palmer in 1988 [42]. Soon the concept was extended to storage-ring colliders by K. Oide and K. Yokoya [43]. The crab-cavity scheme is illustrated in Fig. 16, for the proposed Super-KEKB collider. There are two crab cavities per beam and per IP. Before arriving at the IP, the first crab cavity introduces a transverse deflection of opposite sign for the head and tail of the bunch, in such a way that the collision becomes to first order equivalent to a head-on collision, without any geometric luminosity reduction. The second cavity, on the outgoing side of the IP, cancels the effect of the first cavity.

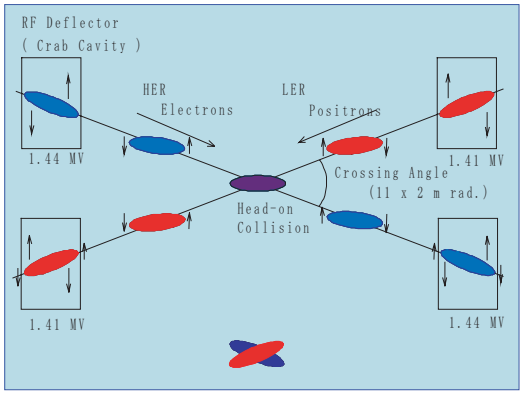

Figure 16: Schematic of crab crossing at SuperKEKB [50].

The first installation of crab cavities in an operating collider is foreseen for the summer of 2006 at the present KEK B factory [51], with only one cavity per ring and different closed orbit for particles in the head and tail of a bunch. Figures 17–19 illustrate some of the fabrication and processing steps for the KEKB superconducing crab cavities. The main motivation for the KEKB and Super-KEKB crab cavities is the prediction by simulations that they will increase the beam-beam tune shift by a factor of two or more [52].

Merits and Issues

The crab cavities combine all the advantages of head-on collisions and large crossing angles, i.e., there is no geo-

Figure 17: Barrel polishing of KEKB crab cavity [53].

Figure 18: Annealing at 700°C for 3 hours of KEKB crab cavity [53].

metric luminosity loss from a large crossing angle, the two beams are easily separated into two magnetic channels, and long-range beam-beam collisions are unimportant.

Crab cavity voltages are much lower than those of an equivalent bunch shortening system. Namely, the voltage required for bunch shortening is

$$V_{\rm rf} \approx \left[\frac{\epsilon_{||,\rm rms}^2 c^3 C\eta}{E_0 e\pi f_{\rm rf}}\right]\frac{1}{\sigma_z^4} \approx \left[\frac{\epsilon_{||,\rm rms}^2 c^3 C\eta}{E_0 e\pi f_{\rm rf}}\right]\frac{\theta_c^4}{0.7^4\ 16\ \sigma_x^{*\,4}}\ , \tag{7}$$

where in the second step we have assumed that the Piwinski angle Θ is held constant at a value of about 0.7. Equation (7) reveals that the bunch-shortening rf voltage scales with the 4th power of the crossing angle and the inverse 4th power of the IP beam size. The voltage can be lowered, to some extent, by reducing the longitudinal emittance (but other limits come from intrabeam scattering and the injectors) and increasing the rf frequency (the voltage scales inversely with the rf frequency).

On the other hand. assuming horizontal crossing, the equivalent crab cavity voltage,

$$V_{\rm crab} = \frac{cE_0\tan(\theta_c/2)}{e2\pi f_{\rm rf,crab} R_{12}} \approx \frac{cE_0}{e4\pi f_{\rm rf} R_{12}}\,\theta_c\ , \tag{8}$$

is linearly proportional to the crossing angle and independent of the IP beam size. The voltage also scales with $1/R_{12}$ where R_{12} is the (1,2) transport matrix element from the location of the crab cavity to the IP. Like the bunch shortening voltage, the crab voltage is inversely proportional to the crab-rf frequency.

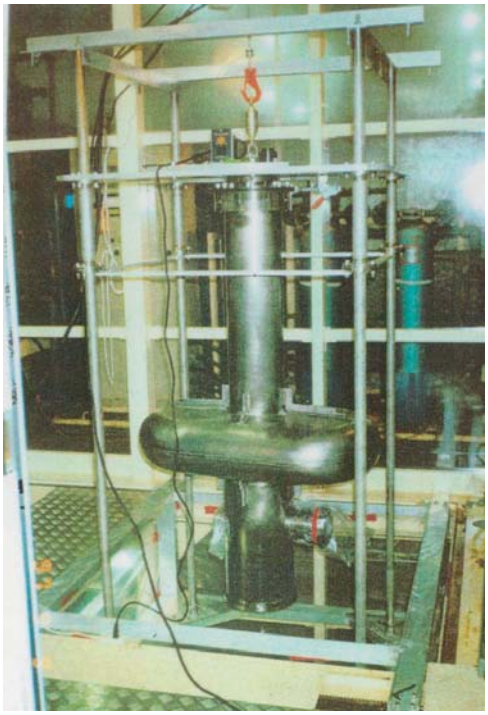

Figure 19: High-pressure water rinsing by 80-bar ultrapure water of KEKB crab cavity [53].

The unfavorable scaling of the bunch-shortening rf voltage is vividly illustrated in Fig. 20, where the voltage required as function of the crossing angle is compared with the corresponding crab voltage. The shortening rf voltage is typically two or three orders of magnitude higher, even if the shortening rf frequency is tripled, to 1.2 GHz, and the longitudinal emittance reduced. Figure 21 shows a zoomed view of the crab-cavity voltage as a function of crossing angle. Table 4 compiles the crab voltages required at three different crossing angles and for three different crab rf freqencies. For crossing angles up to 1 mrad, the 200-MHz system appears practical, but for larger angles it might be advantageous to increase the crab rf frequency to 400 MHz or higher, in order to reduce the total voltage, if permitted by the bunch length.

Table 4: Super-LHC crab-cavity voltage with three different crossing angles and rf frequencies

crossing angle	0.3 mrad	1 mrad	8 mad
800 MHz	2.1 MV	7.0 MV	56 MV
400 MHz	4.2 MV	13.9 MV	111 MV
200 MHz	8.4 MV	27.9 MV	223 MV

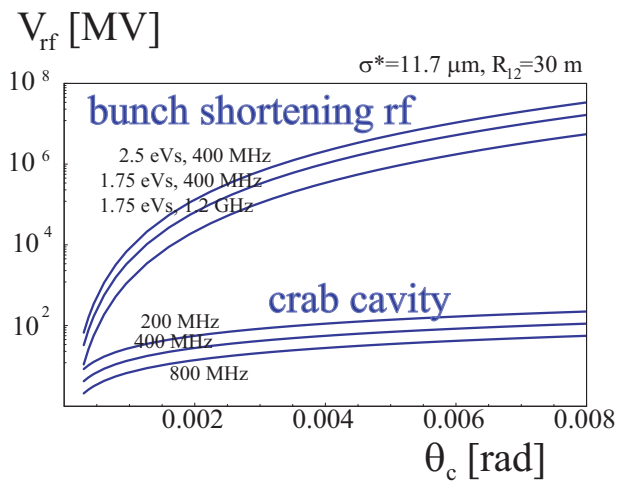

Figure 20: Bunch shortening rf voltage for $R_\Theta = 0.68$ and crab-cavity voltage as a function of the full crossing angle, for different rf frequencies and longitudinal emittances. The curves are computed from Eqs. (7) and (8). An IP beam size of 11.7 μm and $R_{12} = 30$ m from the crab cavity to the IP are assumed [31].

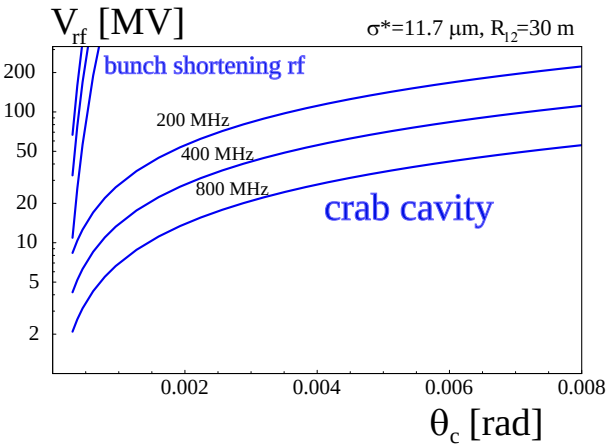

Figure 21: Zoom of Fig. 20 highlighting the crab-cavity voltage required for an LHC upgrade as a function of the full crossing angle, for different rf frequencies and longitudinal emittances. The curves are computed from Eqs. (7) and (8). An IP beam size of 11.7 μm and $R_{12} = 30$ m from the crab cavity to the IP are assumed [31].

However, tight tolerances on crab-cavity phase jitter must be met in order to avoid significant emittance growth. The timing jitter tolerance Δt is related to the IP orbit jitter tolerance $\Delta x_{\max}$ via the relation

$$\Delta t \leq \frac{2\Delta x_{\max}}{n_{\rm IP} c \theta_c} \,. \qquad (9)$$

Earlier in this paper, the orbit jitter tolerance for the LHC was inferred from Alexahin's formula (5), by limiting the emittance growth to 1% per hour without feedback, which yielded a maximum allowed turn-to-turn IP jitter of 0.6 nm. Nearly the same value, namely 0.5 nm, is obtained by scaling the strong-strong simulation results of K. Ohmi [51] to the case of random jitter and the same level of emittance growth.

Table 5 compares the timing tolerance for the Super-LHC crab cavity with those of the crab cavities for KEKB, already produced, for Super-KEKB, under development, and for the ILC, under study. ILC and LHC represent an advance by about one order of magnitude in timing stability compared to the KEKB requirements. The tolerance on the relative beam-beam offset jitter is 4000 times tighter for Super-LHC than for the ILC, but the corresponding timing jitter tolerance only 15 times. The ILC timing tolerance is believed to be within technological reach. For example, the XFEL project at DESY aims at a timing stability of 0.02 ps between different rf systems [54]. It remains to be explored if also the timing stability required for LHC crab cavities is technically feasible.

Table 5: Comparison of phase or timing tolerances for Super-LHC crab cavities with crab cavities for other projects. For KEKB and Super-KEKB , the timing tolerance corresponds to an IP offset of $0.02\sigma_x^*$, for the ILC to $0.2\sigma_x^*$, and for the LHC to one of about $5 \times 10^{-5}\sigma_x^*$.

	KEKB	Super-KEKB	ILC	Super-LHC
σ_x^*	100 μm	70 μm	0.24 μm	11 μm
θ_c	22 mrad	30 mrad	10 mrad	1 mrad
Δt	0.6 ps	0.3 ps	0.03 ps	0.002 ps

Crab-Cavity Layouts

The KEKB crab cavity provides 1.5 MV peak deflecting voltage at 500 MHz. The cavity layout is shown in Fig. 22. It has the geometry of a squashed cell and operates in the TM2-1-0 (x-y-z) mode, which corresponds to the TM110 cylindrical mode. A coaxial coupler is used as the beam pipe. The design shown is for a standard B factory with currents of 1–2 A. For higher current, additional damping is necessary. The total length of the KEKB cell with all damping components is 1.5 m.

The length required for LHC can be estimated by linear scaling with the total voltage. The voltage required depends on the rf frequency. The achievable peak field may also vary with the rf frequency. Nevertheless, we roughly estimate that 2 MV of crab voltage require a crab cavity of length 1.5 m (about the KEKB case), and 20 MV a length of 15 m. Using multi-cell instead of single-cell cavities might reduce the length compared with this simple estimate.

Possible layouts for LHC crab cavities were discussed at a US-LARP meeting in October 2005 [58], where Gupta considered displacing the quadrupoles focusing the two

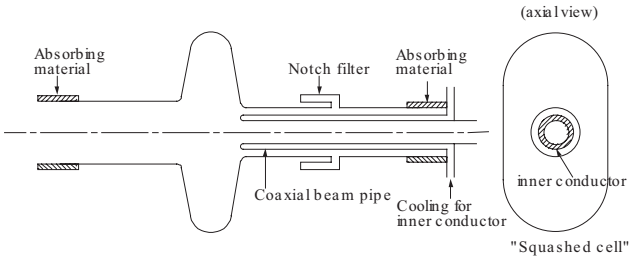

Figure 22: Schematic of squashed cell crab cavity for the KEK B factory [51, 55].

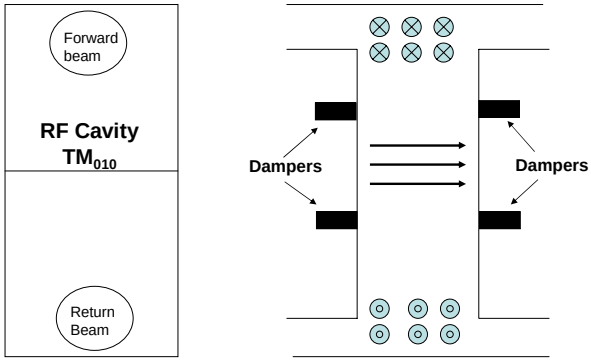

Figure 24: Fundamental-mode two-beam crab cavity [60].

counter-rotating beams so as to minimize the crossing angle (Fig. 23). Over 50 m free space the lateral distance between the two beams is 40 cm for an 8-mrad crossing angle. This is comparable to the larger of the two transverse half-sizes for the KEKB squashed-cell crab cavity. However, one could separate the beams in the plane orthogonal to the plane of crossing (as it is the case for some of the interaction points in the nominal LHC), and then the smaller of the two transverse cavity sizes would be relevant.

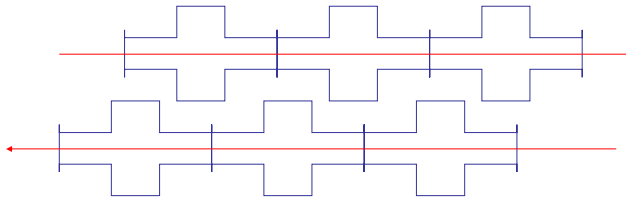

Figure 23: Displaced quadrupoles with the first beam in the quadruple and the counter rotating second beam just outside the coil in a field-free region [59, 60].

Another space-saving measure could be a novel two-beam crab cavity based on the fundamental TM1-1-0 (x-y-z) or TM010 (cyl.) mode, which is illustrated in Fig. 24.

Also induction rf could provide a transversely compact crab-cavity solution.

SUPERBUNCHES AND QCD EXPLORER

Superbunches for LHC Upgrade

The CERN ISR (Intersecting Storage Rings) were the first hadron collider, stored beam currents up to 50 A, and held the world record luminosity of hadron colliders for more than two decades. They operated with coasting (unbunched) beams, which have a number of advantages [61]. In an LHC upgrade, we can produce a quasi-coasting beam if we confine one or several long bunches with a uniform ('flat') density profile by a barrier rf bucket. The collisions of such super-bunches was first proposed by K. Takayama and co-workers for a VLHC [12]. The superbunch collider concept is illustrated schematically in Fig. 25. It can be realized using in induction-rf technology [62].

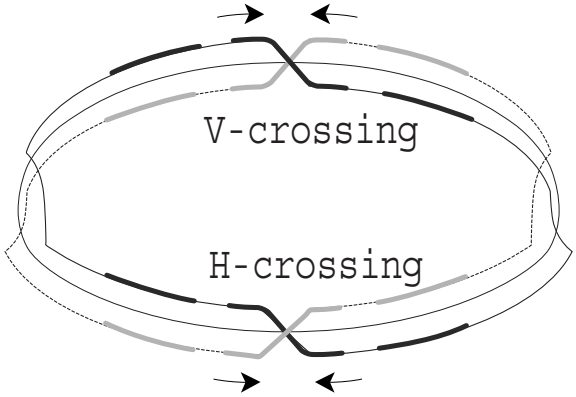

Figure 25: Schematic of super bunches in a high-luminosity collider (K. Takayama et al., Snowmass 2001); alternating crossing in 'x/y' or $45°/135°$ ('inclined hybrid') planes

Example parameters were presented at HHH-2004 [33]. Merits of the superbunch scenario are the negligible heat load from electron cloud, the absence of PACMAN bunches, reduced effect of intrabeam scattering, and a higher luminosity at identical total beam-beam tune shift and lower beam current. The main disadvantage of the superbunch scheme is that the protons are concentrated over a small fraction of the ring circumference, which causes problems for machine protection, for the beam dump, and with the event pile-up in the detector.

Indeed at HHH-2004 the two large experiments ATLAS and CMS issued a joint statement on super-bunches, saying that 'based on the physics motivation for an upgrade of the LHC luminosity by an order of magnitude, it is not seen how in case of the super-bunch scenario, this increase in the luminosity could be exploited by an upgraded ATLAS or CMS detector" [63].

As a consequence, the super-bunch option is no longer considered for the baseline LHC upgrade studies.

QCD Explorer

Super-bunches are, however, retained as option for an electron-proton linac-ring collider based on CLIC-1 (a single drive-beam stage of CLIC) and LHC [64], since the length of proton super-bunches could be tailored to the length of a CLIC bunch train, thereby maximizing the luminosity of such a facility.

Some key points of the QCD Explorer [64] are that (1) it extends the low-x reach of HERA by at least two orders of magnitude, (2) it may provide discoveries that are as fundamental for the QCD as is the Higgs for the electroweak interactions [65], (3) it would be the highest-energy linac-ring collider presently conceivable, (4) the optimum luminosity in excess of 10^{31} cm^{-2}s^{-1} is achieved only with proton super-bunches, and (5) the electron-beam emittances are relaxed compared with the CLIC design values.

The nominally 2808 LHC bunches are spaced at a typical distance of 25 ns and are spread out over a revolution period of about 100 μs. On the other hand, the CLIC beam, in its previous incarnation [66], consisted of 154 bunches spaced by 0.66 ns, and extending over about 100 ns. If we were to collide these two beams, the luminosity would be bound to be low, as only a few bunches of either beam would participate in the collisions. It is difficult to increase the length of the CLIC bunch train. On the other hand, combining some of the 2808 small bunches into a superbunch with a length of about 30 m would produce the ideal counterpart of the CLIC bunch train. Then all CLIC bunches and a significant part of the LHC beam (10%) would contribute to the electron-proton luminosity. The advantage of the proton superbunch is evident from the schematic comparison in Fig. 26.

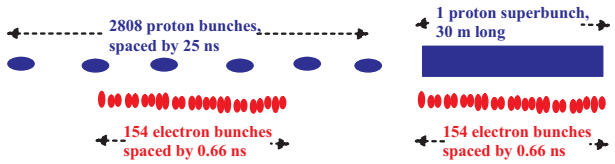

Figure 26: Bunch filling patterns in LHC and CLIC for the nominal LHC (left) and with an LHC superbunch (right) [64].

Possible proton and electron beam parameters are listed in Table 6. The proton parameters are those considered for an LHC superbunch upgrade [2], while the electron beam parameters, especially emittances and IP beta functions, are relaxed compared with the ultimate CLIC target values and could be easily produced by a photo-rf gun without the need of a damping ring. For example, the transverse normalized electron-beam emittance is taken to be 73 μm in both planes. This is more than 100 and 10000 times larger than the 3-TeV CLIC design value of 0.45 μm for the horizontal emittance and of 3 nm for the vertical, respectively. While a smaller electron beam might have its merits, we have assumed, for simplicity, equal beta functions and equal geometric emittances for the two beams. This equality minimizes the nonlinear forces experienced by the proton beam, while at the same time it does not significantly sacrifice luminosity.

Highest luminosity and maximum symmetry are achieved by colliding the two beams head on over a length $l_{\rm IR}$. They can be separated easily by rather weak dipole magnets, since the electron beam-energy is only 1% of the proton energy. It could be advantageous to separate the beams at one side horizontally and at the other vertically, thereby cancelling part of the long-range beam-beam tune shifts [10]. A schematic of the IR layout is shown in Fig. 27. Tentative locations of CLIC-1 on the periphery of the LHC ring are indicated in Fig. 28.

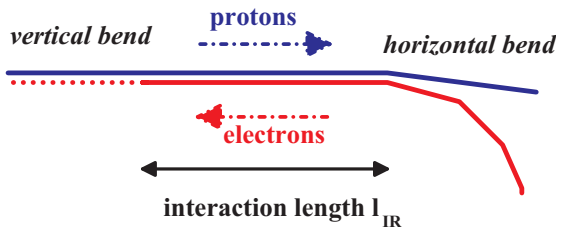

Figure 27: Schematic of IR layout, with horizontal and vertical dipoles for combining and separating the electron and proton beams [64].

Table 6: Beam parameters [64].

parameter	symbol	electrons	protons
beam energy	E_b	75 GeV	7 TeV
bunch population	N_b	4×10^9	6.5×10^{13}
rms bunch length	σ_z	35 μm (Gaussian)	12.4 m (uniform)
bunch spacing	$L_{\rm sep}$	0.66 ns	N/A
number of bunches	n_b	154	1
effective line density	λ	2.0×10^{10} m^{-1}	2.1×10^{12} m^{-1}
IP beta function	$\beta^*_{x,y}$	0.25 m	0.25 m
spot size at IP	$\sigma_{x,y}$	11 μm	11 μm
full interaction length	$l_{\rm IR}$	2 m	
norm. rms emittances	$\gamma\epsilon_{x,y}$	73 μm	3.75 μm
collision frequency	$f_{\rm coll}$	100 Hz	
luminosity	L	1.1×10^{31} cm^{-2}s^{-1}	
beam-beam tune shift	$\xi_{x,y}$	N/A	0.004

SUMMARY AND OUTLOOK

A primary focus of European CARE-HHH studies is the luminosity and energy upgrade of the Large Hadron Collider and its injector complex. Important issues are the choice of beam parameters, and the new IR layout.

Induction-rf technology may contribute to the development of a pulsed long-range beam-beam compensator, to

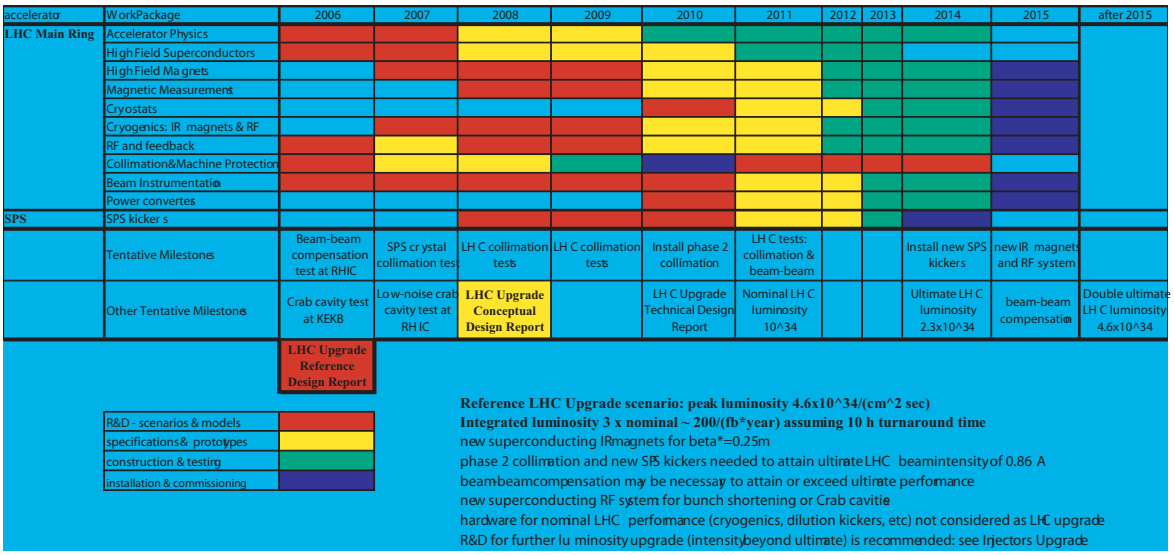

Figure 29: LHC luminosity-upgrade work packages and tentative milestones (F. Ruggiero) [67].

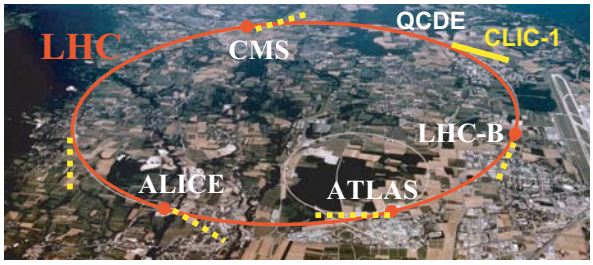

Figure 28: Possible locations of CLIC-1 relative to the LHC tunnel [64].

the optimization of crab cavities, the design of stronger kickers for Super-PS, Super-SPS and Super-LHC, and to the generation of proton super-bunches for a QCD Explorer.

Tentative milestones of future machine studies related to the LHC upgrade comprise:

- 2006: Installation of crab cavities in KEKB; validation of KEKB beam-beam perfomance with crabbing; installation of long-range compensator in RHIC;
- 2007: experiments with three dc beam-beam compensators at SPS; dc compensation experiments with colliding beams in RHIC;
- 2008: the installation of a pulsed compensator at RHIC (LARP); RHIC experiments with pulsed beam-beam compensation; installation of a crab cavity in a hadron machine (also at RHIC?) to validate low rf noise and emittance preservation; studies of electron lenses at RHIC?

Work packages and tentative milestones of the LHC luminosity upgrade programme are summarized in Fig. 29.

ACKNOWLEDGEMENTS

I would like to thank Ulrich Dorda, Wolfram Fischer, Jean-Pierre Koutchouk, Peter McIntyre, Kazuhito Ohmi, Francesco Ruggiero, Walter Scandale, Daniel Schulte, Tanaji Sen, Ken Takayama, Kota Torikai, and Masayoshi Wake for helpful discussions. Special thanks go to Ken Takayama and the Tokyo Institute of Technology for their interest and support.

REFERENCES

[1] The LHC Study Group, "The Large Hadron Collider: Conceptual Design," CERN-AC-95-05-LHC (1995)

[2] O. Bruning et al, "LHC Luminosity and Energy Upgrade: A Feasibility Study," CERN-LHC-PROJECT-REPORT-626 (2002).

[3] Web site *http://esgard.lal.in2p3.fr/Project/Activities/Current/*

[4] Web site *http://care-hhh.web.cern.ch/CARE-HHH/*

[5] Web site *http://lt.tnw.utwente.nl/project.php?projectid=9*

[6] F. Ruggiero, W. Scandale, F. Zimmermann (Eds.), Proc. 1st CARE-HHH-APD Workshop (HHH-2004), CERN-2005-006 (2005).

[7] Web site *http://care-hhh.web.cern.ch/CARE-HHH/LUMI-05/*

[8] J. Strait, private communication, 12 April 2003 (2003).

[9] J. Strait et al., "Towards a New LHC Interaction Region Design for a Luminosity Upgrade," PAC2003 Portland (2003).

[10] F. Ruggiero, F. Zimmermann, "Luminosity Optimization Near the Beam-Beam Limit by Increasing Bunch Length or Crossing Angle," PRST-AB 5:061001 (2002).

[11] F. Ruggiero, G. Rumolo, F. Zimmermann, Y. Papaphilippou, "Beam Dynamics Studies for Uniform (Hollow) Bunches

or Super-Bunches in the LHC: Beam-Beam Effects, Electron Cloud, Longitudinal Dynamics, and Intrabeam Scattering," Proc. RPIA'2002, K. Takayama (ed.), KEK Proceedings 2002-30 (2002)

[12] K. Takayama, J. Kishiro, M. Sakuda, Y. Shimosaki, M. Wake, "Superbunch Hadron Colliders," Phys. Rev. Let. 88, no. 14, 144801-1 (2002).

[13] V. Danilov et al., "Multipacting on the Trailing Edge of Proton Beam Bunches in the PSR and SNS", Proc. Workshop on Instabilities of High-Intensity Hadron Beams in Rings, Upton, N.Y., June 1999, AIP Conf. Proc. 496, p. 315 (1999).

[14] F. Zimmermann, "Two Stream Effects in Present and Future Accelerators," EPAC 2002 Paris (2002).

[15] F. Zimmermann, "Beam Dynamics Challenges for Future Circular Colliders," EPAC04 Lucerne (2004).

[16] J. Bernabeu, et al., "Monochromatic Neutrino Beams," (2005).

[17] E. Malamud et al, "The Pipetron: A Low-Field Approach to a Very Large Hadron Collider," Snowmass 1996.

[18] PS Complex kicker Magnet Systems - Parameters, web site *http://psdata.web.cern.ch/psdata/www/Kickers/psparam.htm* .

[19] E. Gaxiola et al, "Upgrade and Tests of the SPS Fast Extraction kicker System for LHC and CNGS," EPAC'04 Lucerne (2004).

[20] L. Ducimetière et al, "The LHC Injection Kicker Magnet," PAC 2003 Portland (2003).

[21] P. McIntyre, A. Sattarov, "On the Feasibility of a Tripler Upgrade for LHC," CERN Seminar 14.04.2005.

[22] J. Ellis, K.A. Olive, Y. Santoso, V.C. Spanos, "Prospects for Sparticle Discovery in Variants of the MSSM," Physics Letters B603:51, and CERN-PH-TH/2004-131 (2004).

[23] M. Mangano, "Physics Motivation for an LHC Luminosity Upgrade," CARE-HHH LHC-LUMI05 Workshop, Arcidosso, 31 August – 3 September, Italy (2005)

[24] LBNL Superconducting Magnet Program Newsletter, Issue no. 2 (2003).

[25] P. McIntyre, A. Sattorov, "On the Feasibility of a Tripler Upgrade for LHC," in *PAC'05*, Knoxville (2005).

[26] O. Brüning, "Possible Dipole First Layout Options and Challenges," Proc. CARE-HHH LUMI-05 workshop, in [7].

[27] R. De Maria, "LHC IR Upgrade: a Dipole First Option," Proc. CARE-HHH LUMI-05 workshop, in [7].

[28] T. Sen et al, "US-LARP Progress on LHC IR Upgrade," Proc. CARE-HHH LUMI-05 workshop, in [7].

[29] J.-P. Koutchouk, "Possible Quadrupole First Options with $\beta^* \leq 0.25$ m," Proc. CARE-HHH LUMI-05 workshop, in [7].

[30] LHC Upgrade IR Optics Options, web site *http://care-hhh.web.cern.ch/care-hhh/SuperLHC_IRoptics/-IRoptics.html*

[31] F. Zimmermann and U. Dorda, "Progress of Beam-Beam Compensation Schemes," Proc. CARE-HHH LUMI-05 workshop, in [7].

[32] J. Irwin, "Diffusive Losses from SSC Particle Bunches due to Long-Range Beam-Beam Interactions," SSC-233 (1989).

[33] F. Ruggiero, F. Zimmermann, "Possible Scenarios for an LHC Upgrade," Proc. CARE-HHH-APD Workshop, HHH-2004, CERN-2005-006, p. 1 (2005).

[34] Y. Papaphilippou, F. Zimmermann, "Weak-Strong Beam-Beam Simulations for the Large Hadron Collider," PRST-AB 2:104001 (1999).

[35] Y. Papaphilippou and F. Zimmermann, "Estimates of Diffusion due to Long-Range Beam-Beam Collisions," Phys. Rev. Special Topics Accel. Beams 5:074001 (2002).

[36] J. Gareyte, "A 'Modest' LHC Upgrade," Memo to F. Ruggiero and F. Zimmermann, 02.08.2001.

[37] J. Tuckmantel, "RF and Feedback for Bunch Shortening," Proc. CARE-HHH-APD Workhop, HHH-2004, CERN-2005-006, p. 33 (2005).

[38] J.-P. Koutchouk, "Principle of a Correction of the Long-Range Beam-Beam Effect in LHC using Electromagnetic Lenses," LHC Project Note 223 (2000).

[39] J.-P. Koutchouk, "Correction of the Long-Range Beam-Beam Effect in LHC using Electro-Magnetic Lenses," PAC 2001 Chicago (2001).

[40] U. Dorda and F. Zimmermann, " Simulation of LHC Long-Range Beam-Beam Compensation with DC and Pulsed Wires," these proceedings.

[41] U. Dorda et al, "Summary of Working Group 3: Assessment of the Wire Lens Scheme at LHC from the Current Pulsed Power Technology Point of View," these proceedings.

[42] R. Palmer, "Energy Scaling, Crab Crossing, and the Pair Problem," DPF Summer Study Snowmass '88: High Energy Physics in the 1990's, Snowmass, Colorado June 27–July 15 (1988).

[43] K. Oide, K. Yokoya, "The Crab Crossing Scheme for Storage Ring Colliders," Phys. Rev. A40: 315 (1989).

[44] H. Hosoyama et al., "Crab Cavity for KEKB," 7th Workshop on RF Superconductivity, Gif-sur-Yvette (1995).

[45] W. Fischer, M. Blaskiewicz, "Luminosity Increase at the Incoherent Beam-Beam Limit with Six Superbunches in RHIC," Proc. 29th ICFA Advanced Beam Dynamics Workshop HALO'03, Montauk, 19–23 May, 2003, AIP Conf. Proc. 693: 244–247 (2004).

[46] F. Ruggiero et al, "Performance Limits and IR Design of a Possible LHC Luminosity Upgrade Based on Nb-Ti S.C. Magnet Technology," EPAC'04 Lucerne (2004).

[47] J.-P. Koutchouk, J. Wenninger, F. Zimmermann, "Experiments on LHC Long-Range Beam-Beam Compensation in the SPS," EPAC'04 Lucerne (2004).

[48] W. Fischer et al, "Measurement of the Long-Range Beam-Beam Effect at Injection and Design for a Compensator in RHIC," BNL C-A/AP/236 (2006).

[49] Y.I. Alexahin, "On the Emittance Growth due to Noise in Hadron Colliders and Methods of Its Suppression," Nucl. Instr. Meth. A 391, p. 73 (1996).

[50] This picture is taken from M. Masuzawa, "Overview of Super-KEKB," 6th Workshop on a Higher Luminosity B Factory, KEK 16–18 November 2004 (2004).

[51] K. Ohmi, "Study of Crab Cavity Option for LHC," Proc. 1st CARE-HHH-APD Workshop (HHH-2004), CERN-2005-006 (2005).

[52] K. Ohmi et al., “Luminosity Limit due to the Beam-Beam Interactions With or Without Crossing Angle,” PRST-AB 7, 104401 (2004).

[53] Photos are courtesy of K. Oide (2005).

[54] E. Vogel, private communication (2005).

[55] K. Akai et al., Proc. B factories, SLAC-400, p. 181 (1992).

[56] K. Akai, Y. Morita, “Crab Cavity for High-Current Accelerators,” KEK-PREPRINT-2003-123 (2004).

[57] K. Akai and Y. Morita, “New Design of Crab Cavity for SuperKEKB,” Proc. PAC’05, Knoxville (2005).

[58] US-LARP LHC IR Upgrades Workshop, 3–4 October 2005, Pheasant Run, Illinois, 2005, web site *http://larp.fnal.gov/IR2005* .

[59] R. Gupta, “A Quadrupole Design for Crab Cavity Optics,” US-LARP LHC IR Upgrades Workshop, 3–4 October 2005, Pheasant Run, Illinois, 2005.

[60] R. Gupta, “Working Group 3 Summary,” US-LARP LHC IR Upgrades Workshop, 3–4 October 2005, Pheasant Run, Illinois, 2005.

[61] F. Ruggiero et al, “Beam-Beam Interaction, Electron Cloud and Intrabeam Scattering for Proton Super-Bunches,” PAC 2003 Portland (2003).

[62] K. Takayama (Ed.), Proc. RPIA 2002, KEK, October 29–31, 2002, KEK Proceedings 2002-30 (2002).

[63] S. Tapprogge, “Machine-Detector Interface and Event Pile-Up: Super-Bunches Versus Normal Bunches,” in Proc. 1st CARE-HHH-APD Workshop (HHH-2004), CERN-2005-006 (2005).

[64] D. Schulte, F. Zimmermann, “QCD Explorer Based on LHC and CLIC-1,” EPAC’04 Lucerne (2004).

[65] S. Sultansoy, “Linac-Ring Type Colliders: Second Way to TeV Scale,” European Physical Society International Europhysics Conference on High Energy Physics, HEP2003, Aachen, July 17–23, 2003 (2003).

[66] The CLIC Study Team, G. Guignard (Ed.), “A 3 TeV Linear Collider Based on CLIC Technology,” CERN 2000-008.

[67] F. Ruggiero, W. Scandale, “Scenarios for the Luminosity Upgrade in the LHC,” LHC Project Seminar, CERN, 10 November 2005.